

Soft X-ray Induced Production of Neutral Fragments in High-Rydberg States at the O 1s Ionization Threshold of the Water Molecule

Antti Kivimäki,* Tomasz J. Wasowicz, and Robert Richter



Cite This: *J. Phys. Chem. A* 2021, 125, 713–720



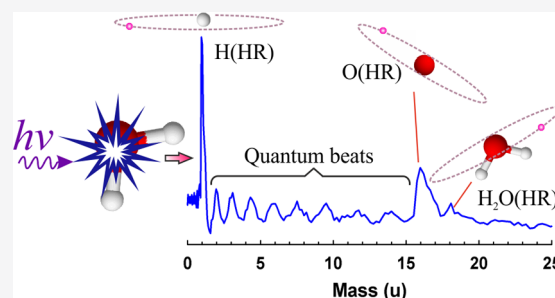
Read Online

ACCESS |

Metrics & More

Article Recommendations

ABSTRACT: Dissociation of water molecules after soft X-ray absorption can yield neutral fragments in high-Rydberg (HR) states. We have studied the production of such fragments by field ionization and ion time-of-flight (TOF) spectrometry. Neutral HR fragments are created at all resonances below the O 1s ionization potential (IP) and particularly within 1 eV above the O 1s IP. The latter effect is due to the recapture of the O 1s photoelectrons into HR orbitals of the molecular water ion after the emission of a fast Auger electron. $\text{H}_2\text{O}^+(\text{HR})$ fragments subsequently dissociate, yielding neutral $\text{H}(\text{HR})$ and $\text{O}(\text{HR})$ fragments, as were found by measuring the TOF spectra by pulsed field ionization. Such measurements were carried out at the O 1s $\rightarrow 4a_1$ and $2b_2$ resonances as well as just above the O 1s IP. The TOF spectra also reveal two series of oscillatory structures that are attributed to quantum beats involving Lyman emission in one of the series and field ionization of $\text{H}(\text{HR})$ fragments in the other series.



I. INTRODUCTION

Interaction of soft X-ray photons with water molecules produces several kinds of particles: electrons, positive ions, negative ions, neutral fragments, and photons of different wavelengths. Photodissociation of water molecules can occur in particularly numerous ways when the incident photon energy approximately equals the ionization potential (IP) of the O 1s shell (539.79(2) eV¹). At photon energies slightly below the O 1s IP, an O 1s electron can be excited to empty molecular (valence) orbitals or to atomic-like Rydberg orbitals. If the used photon energy is larger than the O 1s IP, an O 1s electron can be removed from the molecule; this process is known as O 1s photoionization (or less precisely, inner-shell or core photoionization). The inner-shell hole states decay very quickly—in the femtosecond timescale—by emitting an electron or a soft X-ray photon. In water, the electron emission channel is predominant; the probability of soft X-ray fluorescence for the O K-shell is less than 1%.² The electron emission from core-hole states has a specific name: it is called normal Auger decay when the initial core-hole state is ionized, and resonant Auger decay when the core-hole state is neutral. The final states of the water molecule following resonant and normal Auger decay often have two holes in the valence orbitals and readily dissociate. Owing to these dissociation processes, a multitude of different particles can be observed at the O 1s edge.

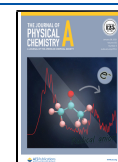
Several different particle yields—measurements of particle's intensity as a function of photon energy—have been reported

in the 1s excitation region of the water molecule, e.g., a total ion yield,³ partial ion yields (of ions such as O^+ , H^+ , O^- , and H^-),⁴ a partial Auger electron yield,⁵ the yield of metastable H atoms,⁶ and Lyman- α and Balmer yields due to excited H atoms.^{7,8} In the present paper, we will show a hitherto unpublished yield of neutral fragments in high-Rydberg (HR) states at the O 1s edge of H_2O , where the term “high-Rydberg” refers to states with the principal quantum number $n \geq 20$. For brevity, we call it the yield of (neutral) HR fragments. The neutral fragments in question are created in excited states below their first ionization energy; they are characterized by a vacancy in the outermost occupied orbital and an electron occupying a high- n orbital. Examples of the species dealt with in this study are an oxygen atom in the $1s^2 2s^2 2p^3 ({}^4S^o) ns$ state or a hydrogen atom in an nl state, $\text{H}(nl)$, where n is of the order of 20–40 in both cases. Expectedly, the yield of HR fragments mostly resembles the yield of metastable hydrogen atoms⁶ because H atoms in HR states are an important subset of metastable atoms. By pulsed field ionization and time-of-flight (TOF) spectrometry, we could determine that H and O

Received: July 29, 2020

Revised: December 19, 2020

Published: January 12, 2021



atoms were produced in HR states after core excitation and core ionization of water molecules.

A quantum beat experiment is often explained using a model system with four energy levels: a ground state $|g\rangle$, two excited states $|a\rangle$ and $|b\rangle$ that are separated by $\hbar\omega_{ab}$ from each other, and a final state $|f\rangle$, see, e.g., ref 9. The model system is subjected to a light pulse that can coherently excite the two closely spaced excited states $|a\rangle$ and $|b\rangle$. If both the excited states can decay via fluorescence emission to the same final state $|f\rangle$, the intensity of the detected signal as a function of time contains two incoherent terms—corresponding to separated decays from the states $|a\rangle$ and $|b\rangle$ —and a coherent or cross term that is modulated by the frequency ω_{ab} . This coherent term is called the quantum beat. In quantum beat experiments, the coherent excitation of the excited states is often achieved with the aid of a laser, but also other methods are possible.¹⁰ Quantum beats have been observed in so-called beam-foil experiments, where monoenergetic beams of H^+ , H_2^+ , and H_3^+ ions were sent through single or double carbon foils and fluorescence due to excited H atoms was observed from short sections at right angles to the beam exiting from the foil.¹¹ When a static electric field was introduced along the beam of excited hydrogen atoms, the intensity of Lyman- α emission was found to show quantum beats as a function of distance from the foil. Knowing the velocity of the exiting atomic beam, each detection point could be correlated to a certain time after excitation. Quantum beats can also appear upon field ionization. Leuchs and Walther¹² populated highly excited $n^2\text{D}$ levels of sodium atoms by stepwise excitation with two dye lasers and applied an electric field to ionize the states a certain time after the laser excitation. A quantum beat signal was observed in the number of field electrons when the time delay between excitation and ionization was varied. In another study of highly excited sodium $n\text{D}$ states, Jeys et al.¹³ varied the slew rates and strengths of the electric fields in their experiment and could elucidate the physics of quantum beats observed in field ionization. More recently, Feynman et al.¹⁴ have studied quantum beats in field ionization of high-Rydberg Rb atoms and presented fully quantum mechanical calculations of the electron's path to ionization. Our TOF spectra obtained with pulsed field ionization show two different series of quantum beats in the same measurement: one of them is related to fluorescence emission from excited H atoms and the other to field ionization of H(HR) fragments.

II. EXPERIMENTAL SECTION

Some of the present authors have recently modified an existing ion time-of-flight spectrometer in order to observe neutral HR fragments from molecular samples.¹⁵ The instrument can be used in the usual multibunch mode of a synchrotron radiation source. Its operation is based on field ionization of HR fragments in a volume shielded electrically by polarized grids from the interaction region where the synchrotron radiation beam crosses a jet of sample molecules. If the interaction between radiation and molecules produces neutral HR fragments, these species can drift into this specific volume (source region in Figure 1), while positive ions created in the interaction region are pulled to the opposite direction using a cation extractor. In addition to the source region, the modified ion TOF mass spectrometer has all the other usual parts: an acceleration region, a field-free drift tube, and a microchannel plate (MCP) detector. The width (2 mm) of the source region determines the mass resolution of the instrument.

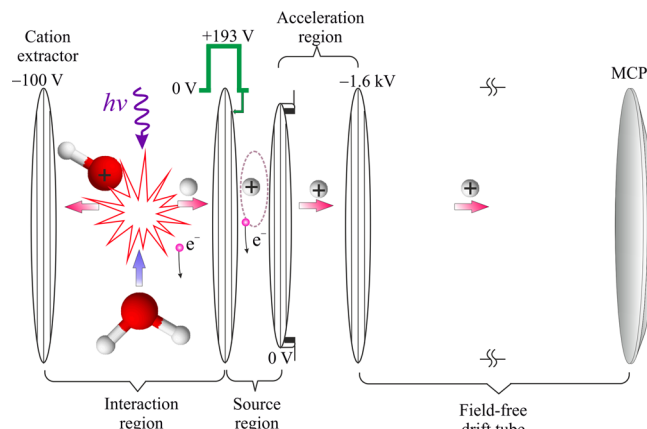


Figure 1. Scheme of the modified ion TOF spectrometer constructed to measure the TOF spectra from neutral fragments in high-Rydberg states, which are field ionized by a high-voltage pulse in the source region.

The modified TOF spectrometer was operated in two different modes to detect neutral HR fragments. A pulsed mode was used to determine the identities and relative intensities of the formed neutral HR fragments. In this mode, the potential in the entrance electrode was varied periodically using a high-voltage pulser, which was driven by a signal generator operating at a 10 kHz frequency (the pulse length was 5 μs). When the potential of the entrance electrode was rapidly raised to a high value (+193 V), field ionization became possible, and a start signal was sent for a TOF measurement. The rise time of the voltage pulse is specified to be less than 25 ns at the maximum output voltage of $\pm 950\text{ V}$, so it should have been even shorter with +193 V. The resulting electric field of $\sim 970\text{ V cm}^{-1}$ in the source region lowered the ionization energy of the species by $\sim 190\text{ cm}^{-1}$ (as calculated from the equation $\Delta E = 6\sqrt{F}$, where E is given in cm^{-1} and F is given in V cm^{-1}).¹⁶ This field can ionize H(n) atoms with $n \geq 24$ and O atoms in the $2s^2 2p^3(^4\text{S}^o)ns/nd$ states with $n \geq 25$ or 24.¹⁷ An ion hitting the MCP detector gave a stop signal. The start and stop signals were fed into a time-to-digital converter system (ATMD-GPX from ACAM), with a time resolution of 82 ps.

The operation potentials of the TOF spectrometer were selected according to the simulations,¹⁵ but they approximately followed the Wiley–McLaren space focusing conditions. The potentials of the electrodes can also be set at suitable constant values to collect the yield of field-ionized HR fragments, while positive ions created in the interaction region are blocked. We achieved this by grounding the electrodes on both sides of the source region while keeping the drift tube at -1.6 kV and cation extractor at -100 V (see Figure 1); this potential configuration allowed the detection of field-ionized species created in the acceleration region. The electric field of 3.2 kV cm^{-1} could field ionize H(n) atoms with $n \geq 18$ and O atoms in the $2s^2 2p^3(^4\text{S}^o)ns/nd$ states with $n \geq 19$.¹⁷ A yield measurement performed in these conditions also contained contributions from metastable atoms that were not field ionized and from VUV and soft X-ray photons that the MCP detector can detect. The total contribution of those three kinds of particles was measured separately by preventing all positive ions from entering the drift tube. We did that by setting the potential to +250 V in the drift tube while keeping the other potentials the same.

The measurements were performed at the Gas-Phase Photoemission beamline¹⁸ at the Elettra synchrotron radiation facility in Trieste, Italy. The storage ring was operated in the multibunch mode with a 2 ns interval between electron bunches. An effusive beam of water vapor from a hypodermic needle was introduced into the interaction region, resulting in an ambient pressure of 7.0×10^{-6} mbar in the vacuum chamber during most measurements. The pressure in the interaction region was estimated to be 10–50 times higher.

III. RESULTS AND DISCUSSION

III.1. Yield of Neutral HR Fragments. Figure 2 shows the sum yield (black dots) of field-ionized HR fragments,

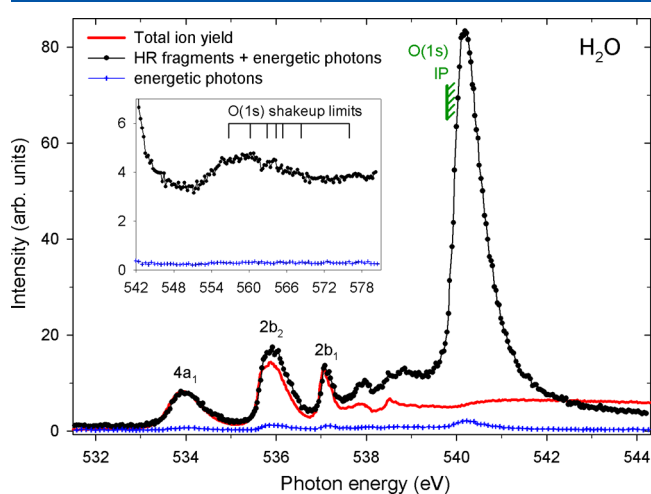


Figure 2. Different particle yields measured across the O 1s edge of the water molecule. The most intense resonances and O 1s ionization potential are indicated. The inset shows the results in the region of core–valence double excitations and O 1s shake-up limits.

(nonionized) metastable neutrals, and energetic photons measured across the O 1s excitations and the O 1s IP. The contribution of the latter two groups of particles was measured separately in similar conditions (pressure, a measuring time of 10 s, and a photon energy resolution of 0.2 eV) by preventing positive ions from entering the drift tube (hence, field-ionized HR fragments were not measured). That result is shown by a blue curve in the bottom of the graph; we see that the contribution of metastable neutrals and energetic photons to the black curve is negligible at most photon energies. Also shown is the total ion yield (red solid curve), which was recorded in a separate measurement using a higher photon resolution of about 70 meV. It is scaled at the same height with the black curve around 534 eV photon energy. The inset shows two of the yields in the region of the core–valence double excitations and thresholds for O 1s shake-up photoionization.

The comparison of the HR yield to the total ion yield reveals that the production of HR fragments is slightly enhanced, in relative terms, at the second resonance (O 1s \rightarrow 2b₂). The difference between the HR yield and total ion yield increases when the photon energy approaches the O 1s IP—in this region, the O 1s electron is excited to increasingly higher Rydberg orbitals—and rises dramatically just after the core ionization threshold.

The production of neutral HR fragments has been described in some detail in earlier papers,^{15,19} but the mechanisms are summarized here for the sake of completeness. As a starting

point, we assume that a neutral HR fragment can be formed following the (resonant or normal) Auger decay of the core-hole state, only if the parent molecular ion has an electron in an HR orbital before dissociation. The core-excited states below the O 1s IP predominantly decay via spectator resonant Auger decay, where a valence electron fills the core hole while another valence electron is emitted. The electron originally promoted to an unoccupied valence or Rydberg orbital acts as a spectator, occupying the same orbital after resonant Auger decay. However, there is possibility that the electron jumps to a higher orbital during the decay; this is called a shake-up process. Shake-up processes to different orbitals have different probabilities according to the overlaps of the wave functions of the involved orbitals before and after the resonant Auger decay. Armen²⁰ has calculated for atoms that the higher is the principal quantum number n of the promoted electron in the core-excited state, the more likely become shake-up processes toward HR orbitals in resonant Auger decay. If shake-up processes follow similar trends in molecules, we may expect (valence)⁻²HR¹ states of the molecular ions to be created most abundantly just below the core (O 1s) ionization potential. When such states dissociate, a neutral fragment can receive an electron in an HR orbital, forming a (valence)⁻¹HR¹ state. Such a state can be field ionized, and we can observe the event as the resulting ion hits the MCP detector.

The mechanism to explain the production of molecular HR states above the O 1s IP is based on the post-collision interaction²¹ and electron recapture processes embedded in it. When the photon energy is just above the core IP, a slow 1s electron can be ejected into the continuum. In molecules containing light atoms, the resulting core hole is typically filled by normal Auger decay, whereby a fast Auger electron is emitted. The Auger electron can “overtake” the photoelectron, and the two electrons can exchange energy in the field of the ionized molecule: the photoelectron loses energy and the Auger electron gains energy (these effects are clearly seen in the core photoelectron and Auger electron spectra measured at photon energies close to the core IP). The energy loss of the photoelectron can be so large that the molecular ion can recapture the electron. The electron can end up in an HR orbital of the singly ionized parent molecule: electronic states of type (valence)⁻²HR¹ can again be reached. Their dissociation can produce neutral HR fragments that can be field ionized. Figure 2 shows that recapture processes populating HR states of the water ion are very efficient just above the O 1s IP of water. The above-described mechanisms can also be used to explain the production of HR fragments in the photon energy range of 548–575 eV, where core–valence double excitations and thresholds for O 1s shake-up ionization are located.

Harries et al.⁶ have measured the yield of metastable H atoms from water by using two MCP detectors shielded from the interaction region by two polarized grids and exploiting the timing structure of the pulsed synchrotron radiation source. They separated the intensity of the metastable atoms from that of fluorescence by looking at different time regions; fluorescence reached the detector within 100 ns of the ring pulse, while metastable atoms arrived in the range of 1–2 μ s. The metastable H atoms with lifetimes longer than 2 μ s include H(2s) and various H(HR) states. The authors did not find any evidence from other neutral species (O, OH, H₂, or H₂O) in their measurements. On the other hand, Hikosaka et al.²² have observed that molecular water ions in HR states,

produced in recapture processes, can dissociate into excited O and OH fragments, which in turn can decay by electron emission (i.e., autoionization). That process can be interpreted as electron reemission following photoelectron recapture.

III.2. Time-of-Flight Spectra of Field-Ionized HR Fragments. Pulsed field ionization TOF spectra were measured using long acquisition times at the O 1s \rightarrow 4a₁ and 2b₂ resonances as well as at the photon energy of 540.35 eV, which corresponds to the maximum of the HR fragment yield in Figure 2. These spectra are shown in Figure 3a. The

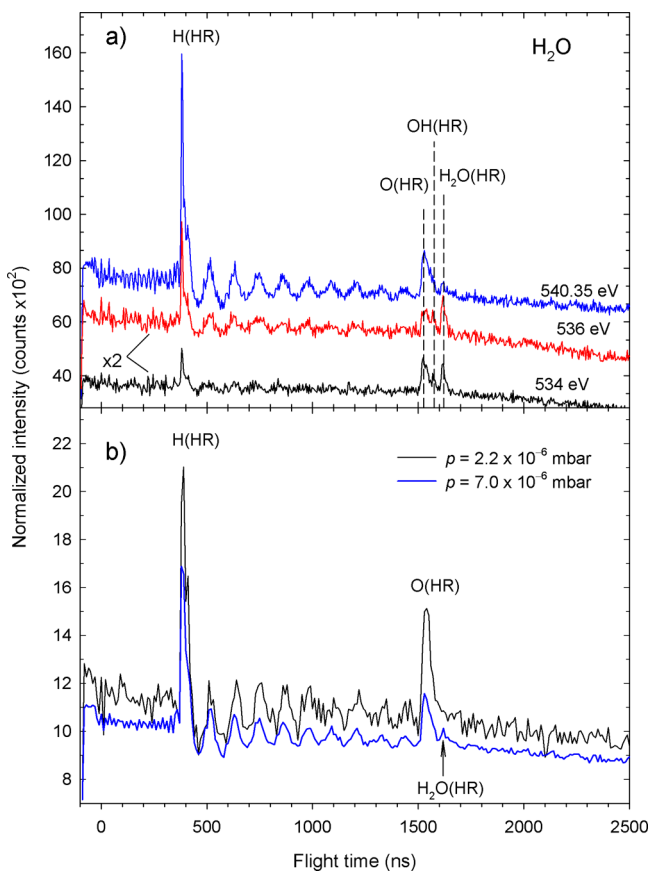


Figure 3. (a) TOF spectra of field-ionized HR fragments measured at the photon energies of 534.0 eV (O 1s \rightarrow 4a₁ resonance), 536.0 eV (O 1s \rightarrow 2b₂ resonance), and 540.35 eV (just above O 1s IP). The flight times are referred to the arrival of HV pulses at 0 ns. The oscillatory structures in the time ranges of 0–350 and 500–1500 ns are discussed in the text. The measuring time of each spectrum was 4 h. (b) TOF spectra of field-ionized HR fragments measured at the photon energy of 540.35 eV at two different pressures. They have been normalized to the measuring time and pressure of the vacuum chamber.

intensity scale refers to the uppermost spectrum and results from binning events in 4 ns wide time windows. The other spectra have been normalized with respect to the uppermost spectrum using the measured photon flux ratios. The TOF spectra have been mass calibrated by assuming that the peaks at 382 ns and 1.62 μ s are due to H(HR) and H₂O(HR), respectively, and by using the equation given in ref 23. The calculated positions for the O(HR) and OH(HR) peaks, shown with dashed lines in Figure 3a, agree well with the other features observed in the TOF spectra. The observed position of the O(HR) peak agreed with that of the corresponding peak

in the CO₂ molecule, measured under similar experimental conditions.²³ We also measured a field ionization TOF spectrum at the photon energy of 540.35 eV using a lower pressure of 2.2×10^{-6} mbar in order to find out whether the prominent oscillations between the H(HR) and O(HR) peaks depended on the pressure. That low-pressure spectrum is compared in Figure 3b to the uppermost TOF spectrum of panel a; the intensity of the latter spectrum has been divided using the ratios of measuring times and pressures of the vacuum chamber. The data in Figure 3b have been binned in 10 ns wide windows.

We can see in Figure 3a that the intensity ratio between the H(HR) and O(HR) fragments increases when going from the 4a₁ resonance to the 2b₂ resonance. This behavior is in agreement with the corresponding intensity ratios of the H⁺ and O⁺ ions in the partial ion yield measurements.⁴ The absolute number of H(HR) and O(HR) greatly increases in the top spectrum of Figure 3a, which is not surprising, considering that the yield of all neutral HR fragments has a maximum at that photon energy (Figure 2). The normalized intensity of both H(HR) and O(HR) decreased when the pressure was lowered, but that of O(HR) decreased proportionally more (Figure 3b). We suggest tentatively that at the higher pressure, more O(HR) fragments were depleted in collisions on the way from the interaction region to the source region because O(HR) fragments are on average slower than H(HR) fragments. With hindsight, it would have been better to perform the experiments at a lower ambient pressure than 7.0×10^{-6} mbar.

Apart from the H(HR) and O(HR) peaks, there are traces of OH(HR) fragments in the two TOF spectra measured at the below-edge resonances. Surprisingly, the parent molecule also appears in the field ionization mass spectra. It is stronger in the measurements performed at the core excitations than above O 1s threshold. To explain the H₂O(HR) peak, we must have water molecules in (valence)⁻¹HR¹ states in the source region. In the case of core excitations, this could only happen if the core-excited states decayed via soft X-ray emission to valence-excited states and during the decay, the electron in the 4a₁ or 2b₂ orbital shook up to an HR orbital. Such transitions are very unlikely and they occur in the femtosecond timescale, so the molecules are in the interaction region when they happen. The lifetimes of the (valence)⁻¹HR¹ states can be long enough (hundreds of nanoseconds or even greater) for such species to drift into the source region before their de-excitation. However, it is very difficult to explain why a peak originating from soft X-ray fluorescence (H₂O(HR)) would be as intense as peaks originating from resonant Auger decay (H(HR) and O(HR)). It is more likely that the H₂O(HR) peak is electron induced. Photoelectrons and Auger electrons emitted from sample molecules can enter the source region and excite neutral molecules to HR states. Field ionization could then create H₂O⁺ ions that are detected. If this scheme is correct, the height of the H₂O(HR) peak should follow the photoionization cross section, which seems to hold true: the H₂O(HR) peak is the highest at the O 1s \rightarrow 2b₂ resonance. Furthermore, if H₂O(HR) was electron induced, the intensity of the corresponding peak should depend quadratically on the pressure because its appearance relies on two consequent events. There is indeed no evident H₂O(HR) peak in the TOF spectrum measured at the lower pressure in Figure 3b. That spectrum does not have good statistics, but it nevertheless shows the oscillations between the H(HR) and O(HR) peaks,

some of which have similar amplitudes to the $\text{H}_2\text{O}(\text{HR})$ peak in the spectrum measured at the higher pressure in Figure 3b. Note also that the normalized intensities of $\text{H}(\text{HR})$ and $\text{O}(\text{HR})$ increased with the decrease in pressure; the behavior of $\text{H}_2\text{O}(\text{HR})$ was opposite. Pressure dependence of the $\text{H}_2\text{O}(\text{HR})$ signal gives further evidence that $\text{H}_2\text{O}(\text{HR})$ was electron induced.

The OH^+ ion is a common photodissociation product at the O 1s edge of water,⁴ and excited neutral OH fragments have been observed after recapture processes.²² In Figure 3a, the intensity ratio between the $\text{H}_2\text{O}(\text{HR})$ and $\text{OH}(\text{HR})$ peaks is similar at the $4a_1$ and $2b_2$ resonances, whereas that between the $\text{H}_2\text{O}(\text{HR})$ and $\text{O}(\text{HR})$ peaks changes. This could indicate that $\text{OH}(\text{HR})$ mostly results from electron-induced processes, where $\text{H}_2\text{O}(\text{HR})$ molecules dissociate into $\text{OH}(\text{HR})$ before the arrival of the HV pulse. In fact, we cannot find convincing evidence in our spectra that there would be a photon-induced contribution to the $\text{OH}(\text{HR})$ peak. If it exists, it is much lower than those for $\text{H}(\text{HR})$ and $\text{O}(\text{HR})$.

Ionization of HR fragments by electrons is worth considering because electrons can enter the source region. If electrons were created without initial velocity in the center of the interaction region, it would take only about 1.5 ns for them to reach the source region (we assume that the HV pulse is on at +193 V and that there is a homogeneous electric field in the interaction region). In reality, photoelectrons and Auger electrons have substantial kinetic energies, but that does not affect our conclusion: If electrons coming from the interaction region ionize HR fragments in the source region, the resulting ion signal would appear within the same peaks of the TOF spectrum as the ion signal directly caused by field ionization. Photoelectrons and Auger electrons can enter the source region also when there is no HV pulse (which is the case for 95% of the time). If they ionized HR fragments effectively, they would rapidly quench HR fragments in the source region.

III.3. Quantum Beats in Pulsed Field Ionization TOF Spectra. The uppermost TOF spectrum in Figure 3a shows a distinct series of oscillations between the $\text{H}(\text{HR})$ and $\text{O}(\text{HR})$ peaks. The period of these oscillations appears constant, ~ 115 ns. Some weak features beyond the $\text{O}(\text{HR})$ peak also belong to this series; for instance, two of them are in the range of 2100–2300 ns. An inspection of that TOF spectrum in the range of 0–350 ns reveals several narrow peaks, some of which also appear at the same positions in the spectrum measured at the O 1s \rightarrow $2b_2$ resonance. The interval between many of those peaks is ~ 20 ns. The two series appear superimposed in the range of 450–700 ns. A Fourier transform analysis of the oscillations revealed frequencies at about 8.8 MHz (114 ns) and 49 MHz (20 ns); the results are shown in Figure 4.

The small peaks at shorter flight times than the $\text{H}(\text{HR})$ peak cannot arise from ions created in field ionization because corresponding signals are detected before the fastest possible ionic fragment, the proton. MCP detectors can also detect photons of sufficiently short wavelengths. The detector of this particular ion TOF spectrometer has previously detected Lyman radiation due to excited H atoms.²⁴ Such emission usually takes place in the nanosecond timescale. Characteristics of Lyman emission change in the electric field. For instance, hydrogen atoms can be created in the metastable $\text{H}(2s)$ state, whose lifetime is 0.14 s in field-free conditions. A very low static electric field in the range of 10^{-2} V cm^{-1} can already mix the $\text{H}(2s_{1/2})$ and $\text{H}(2p_{1/2})$ states and shorten the lifetime of the $\text{H}(2s)$ states through Lyman- α emission.²⁵ The lifetime

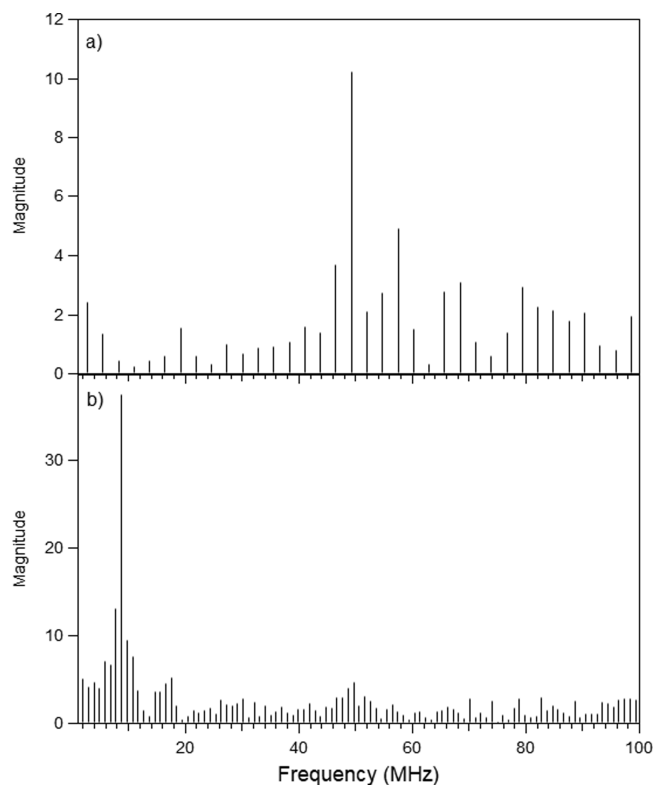


Figure 4. Fourier transforms of the field ionization TOF spectrum measured at the photon energy of 540.35 eV in the flight time ranges of (a) 5–365 ns and (b) 460–1430 ns. The maxima are located at ~ 49 MHz in panel (a) and at ~ 8.8 MHz in panel (b).

depends on the strength of the electric field.²⁶ In our experiments, the $\text{H}(2s_{1/2})/\text{H}(2p_{1/2})$ mixing occurred in the interaction region even without the voltage pulse because the electric field was then about 91 V cm^{-1} . This field increased to ~ 270 V cm^{-1} with the arrival of the HV pulse.

We believe that the abrupt change of the electric field created conditions for quantum beats. Our experimental arrangement was rather contrary to that in the beam-foil experiments,¹¹ where a beam of fast, monoenergetic excited H atoms entered a region of static electric field. In our experiments, excited H atoms moved in random directions in the interaction region, whereas the electric field was rapidly changed from one value to another. Looking at the uppermost TOF spectrum in Figure 3a, we can see that the baseline intensity does not change appreciably when the voltage pulse arrives at time = 0 ns. That intensity probably contained contributions from several Lyman decay channels (as well as from randomly created ions). Some individual channels may increase in strength, while other channels may decrease when the electric field changes. However, the arrival of the HV pulse provided a way to change the population of the excited states coherently at a precise moment. The main effect of the HV pulse could then be that it “switched on” the coherent term in the intensity equation (see Section I), bringing it into the observation window of our experiment. The observation of an oscillating peak structure just above 0 ns in the uppermost spectrum of Figure 3a agrees qualitatively with that suggestion, even though there are some small ripples in the intensity even before 0 ns. Quantum beats related to fluorescence emission do not stand out in the spectrum measured at the lower pressure in Figure 3b. This could have been due to statistics

because their absolute intensities are expected to be almost 20 times smaller than those in the spectrum measured at the higher pressure.

However, the beat period of ~ 20 ns seen in the uppermost spectrum of Figure 3a does not agree with the $2s_{1/2}-2p_{1/2}$ splitting of the H energy levels, which should give a beat period in the range of 0.6–0.9 ns in an electric field below 270 V cm^{-1} .¹¹ Statistics and time resolution of our experiment were not sufficient to resolve such a short quantum beat period, but the emission from the $2s_{1/2}-2p_{1/2}$ states may have contributed to the background of the measured TOF spectra. The observed beat frequency should thus originate from the energy difference between some other energy levels. Another pair of states that could be associated with high fluorescence intensity results from the mixing between the $3p_{3/2}$ and $3d_{3/2}$ states. The $3d_{3/2}$ state could become significantly populated in fluorescence from higher np states, as it is the lowest d state. The energy difference between the $3p_{3/2}$ and $3d_{3/2}$ states is smaller than 49 MHz in field-free conditions,¹⁷ but it is calculated to increase to about 135 MHz in the field of $\sim 90 \text{ V cm}^{-1}$ (for $|m_l| = 1/2$) and even higher in the field of $\sim 270 \text{ V cm}^{-1}$.²⁷ In reality, we do not accurately know the electric field in the interaction region because field penetration from the acceleration region quite certainly decreased it from the nominal value. Consequently, we cannot assign the quantum beats with the period of 21 ns to specific excited states of H atoms using the available information of the experimental conditions. In our experiments, electron field-influenced Lyman emission could also have taken place in the source region. However, excited H atoms should have been far more numerous in the interaction region, where they were originally created, than in the source region, where some H atoms in metastable or high-Rydberg states drifted.

In the quantum beat field ionization experiments of highly excited $n^2\text{D}$ levels of sodium atoms, the fine structure splitting, which was responsible for the quantum beats, was measured to be in the range from 10 to 3 MHz for $n = 21$ to 31.¹² The beat frequency of 8.8 MHz observed for the oscillations between the H(HR) and O(HR) peaks in our TOF spectrum (Figure 3b) occurs within the same range. We attribute those oscillations to field ionization of H(HR) states, even though we cannot assign the observed beat frequency to energy differences between specific energy levels of hydrogen atoms. Our experiment is very different from those used in refs 12–14, which combined laser excitation of Na or Rb atoms with field ionization. Laser excitation could create coherently populated states before field ionization. In our study, H(HR) fragments that result from the dissociation of excited molecular water ions are individual particles in different electronic states and not coherent. The coherent population of states, which is required for quantum beats to appear, should be formed by the action of the quickly rising HV pulse. We explain in the following how quantum beats could appear in our experiments.

The wave functions and energy level structure of the hydrogen atom in the electric field (the Stark structure) can be described by the principal quantum number n , magnetic quantum number m , and parabolic quantum numbers n_1 and n_2 , which obey the relation $n_1 + n_2 + |m_l| + 1 = n$.²⁸ The Stark effect mixes the energy levels of the same magnetic quantum number and produces a complex set of many avoided level crossings when the electric field is increased.¹⁴ An electron that begins in a single state at low field will spread out over multiple states as it passes through avoided crossings until field

ionization.²⁹ Feynman et al.¹⁴ and Gregoric et al.²⁹ have performed quantum mechanical calculations for the spreading of the amplitude using hydrogen-like wave functions in the parabolic basis and compared them with the experimental results of Rb atoms in high-Rydberg states. The calculations show that the spreading of amplitude can become very complicated if there are several avoided crossings before field ionization. However, it also seems possible that the amplitude can remain concentrated in two states (see Figure 1a in ref 29). The avoided crossings provide a means to populate coherently two (or more) energy states. Feynman et al.¹⁴ considered a model experiment with two pairs of states that undergo just two avoided crossings when the electric field is ramped up and described how quantum beats can arise when the electrons field ionize. The reader is referred to their study for the details of the mechanism. The cited studies^{12–14,29} deal with quantum beats observed in electron detection. However, the same mechanism is also valid for quantum beats observed in ion detection because field ionization of a hydrogen atom in an HR state produces simultaneously a free electron and a proton. The quantum beat structure in our field ionization TOF spectra could thus be understood if the quickly ramped up electric field gave rise to two predominant and coherently populated electron states that field ionized.

We believe that many different H(HR) states are populated after recapture processes when the photon energy is set just above the O 1s threshold. When those states are field ionized, one could expect that several different beat frequencies appear simultaneously and that the sum of their individual contributions would effectively flatten the observed spectrum. The appearance of a dominant quantum beat frequency (at 8.8 MHz) could indicate that energy differences between the energy levels do not depend much on the specific quantum numbers of the $H(n, m, n_1, n_2)$ states, when n is rather large, or that we have a situation where field ionization of some specific $H(n, m, n_1, n_2)$ states is far more important than that of the other H(HR) states. The latter option seems more likely since field ionization probabilities of H atoms in high-Rydberg states can vary tremendously as a function of n in a given electric field.³⁰

Quantum beats were not considered in our previous study of neutral HR fragments in the CO_2 molecule,²³ but weak oscillations can be distinguished above the O(HR) peak in some of the field ionization TOF spectra (see Figures 3 and 44 in ref 23). An inspection of the spectra in the time domain revealed a beat period of ~ 120 ns, which is not conclusively different from that observed in the present study (114 ns).

Ion TOF spectrometers are commonly operated by pulsed extraction fields. What was particular in the present experiments that made the quantum beats visible? First, we blocked the flow of positive ions from the interaction region. If such ions are collected, their rates are typically several orders of magnitude higher than those of the field-ionized HR fragments. Second, one of our experiments was performed in conditions where the production of excited H atoms seems exceptionally high, namely, just above the O 1s edge of the water molecule.

The present work demonstrates that quantum beats can be studied by time-of-flight spectrometry in combination with pulsed field ionization. The present TOF spectrometer could be improved rather easily to function better in quantum beat experiments. For instance, one could mount double meshes to limit penetration of the electric field from the acceleration region to the source region, which would allow more

quantitative information to be obtained from the states involved in quantum beats. The cation extractor could be mounted in another direction, eliminating or at least decreasing the flow of electrons from the interaction region toward the source region of the TOF spectrometer. That should decrease electron-induced processes in field ionization TOF spectra.

IV. CONCLUSIONS

We have studied the production of neutral HR fragments at the O 1s edge of the water molecule. Although HR fragments are neutral, they can rather easily be observed with our modified ion TOF spectrometer that has a specific section to field ionize neutral HR fragments either with a static or pulsed electric field. The yield measurement of neutral HR fragments can be done with a static electric field. It is a robust experiment and can be performed relatively fast (we used 10 s per energy point). We observed neutral HR fragments at all core excitations below the O 1s IP and at core–valence double excitations above the O 1s IP. Particularly, many of these rather exotic species are produced when the exciting photon energy exceeds the O 1s IP by few tenths of an electronvolt. This is the energy region where a molecular water ion can recapture a slow O 1s photoelectron in one of its HR orbitals after the emission of a fast Auger electron. Subsequent dissociation of the $\text{H}_2\text{O}^+(\text{HR})$ ion yields atomic species, H(HR) and O(HR), which were verified by measuring the TOF spectra of the HR fragments by pulsed field ionization. The TOF spectra also reveal the molecular species OH(HR) and $\text{H}_2\text{O}(\text{HR})$, which were interpreted to arise from electron-induced excitation of neutral water molecules into HR states.

Additionally, our field ionization TOF spectra showed two series of periodic features that cannot arise from simple field ionization of neutral HR fragments. We attribute them to quantum beats occurring in Lyman emission in one of the series (period ≈ 20 ns) and field ionization of H(HR) fragments in the other series (period ≈ 114 ns). The rapid increase in the electric field used to field ionize neutral HR fragments caused sudden changes in the mixing and evolution of the quantum states of the highly excited H atoms. Apparently, pairs of excited states became coherently excited, and their subsequent decay via fluorescence or field ionization led to conditions required for quantum beats. We cannot assign the observed quantum beats to definite pairs of excited states as the electric fields in the different sections of the TOF spectrometer were not exactly known. However, possible candidates for triggering quantum beats in fluorescence are the $(3p_{3/2}-3d_{3/2}) \rightarrow 1s$ transitions. The quantum beats related to field ionization involved much higher n quantum numbers, most likely in the range of 25–40.

AUTHOR INFORMATION

Corresponding Author

Antti Kivimäki – Nano and Molecular Systems Research Unit, University of Oulu, 90014 Oulu, Finland; MAX IV Laboratory, Lund University, 22100 Lund, Sweden; orcid.org/0000-0003-0753-8164; Phone: +46-702-638383; Email: antti.kivimaki@maxiv.lu.se

Authors

Tomasz J. Wasowicz – Division of Complex Systems Spectroscopy, Institute of Physics and Computer Science,

Gdańsk University of Technology, 80-233 Gdańsk, Poland; orcid.org/0000-0001-5179-4021

Robert Richter – Elettra Sincrotrone Trieste, 34149 Trieste, Italy; orcid.org/0000-0001-8585-626X

Complete contact information is available at: <https://pubs.acs.org/10.1021/acs.jpca.0c06940>

Notes

The authors declare no competing financial interest.

ACKNOWLEDGMENTS

We are grateful to the Elettra Sincrotrone Trieste for providing beamtime no. 20155267. The stay of T.J.W. at Elettra was financially supported by COST Action CM1204 XLIC (COST-STSM-CM1204-32611). Assistance of the staff of the Sincrotrone Trieste is also gratefully acknowledged.

REFERENCES

- (1) Sankari, R.; Ehara, M.; Nakatsuji, H.; Senba, Y.; Hosokawa, K.; Yoshida, H.; De Fanis, A.; Tamenori, Y.; Aksela, S.; Ueda, K. Vibrationally Resolved O 1s Photoelectron Spectrum of Water. *Chem. Phys. Lett.* **2003**, *380*, 647–653.
- (2) Krause, M. O. Atomic Radiative and Radiationless Yields for K and L Shells. *J. Phys. Chem. Ref. Data* **1979**, *8*, 307–327.
- (3) Hiraya, A.; Nobusada, K.; Simon, M.; Okada, K.; Tokushima, T.; Senba, Y.; Yoshida, H.; Kamimori, K.; Okumura, H.; Shimizu, Y.; et al. H_2^+ Formation from H_2O^+ Mediated by the Core-Excitation Induced Nuclear Motion in H_2O . *Phys. Rev. Lett.* **2001**, *63*, No. 042705.
- (4) Stolte, W. C.; Sant'Anna, M. M.; Öhrwall, G.; Dominguez-Lopez, I.; Piancastelli, M. N.; Lindle, D. W. Photofragmentation Dynamics of Core-Excited Water by Anion-Yield Spectroscopy. *Phys. Rev. A* **2003**, *68*, No. 022701.
- (5) Hjelte, I.; Piancastelli, M. N.; Fink, R. F.; Björneholm, O.; Bässler, M.; Feifel, R.; Giertz, A.; Wang, H.; Wiesner, K.; Ausmees, A.; et al. Evidence for Ultra-Fast Dissociation of Molecular Water from Resonant Auger Spectroscopy. *Chem. Phys. Lett.* **2001**, *334*, 151–158.
- (6) Harries, J. R.; Gejo, T.; Honma, K.; Kuniwake, M.; Sullivan, J. P.; Lebeck, M.; Azuma, Y. Long-Lived, Highly Excited Neutral Hydrogen Atom Production Following Oxygen 1s Photoexcitation of Gas-Phase Water Molecules. *J. Phys. B: At., Mol. Opt. Phys.* **2011**, *44*, No. 095101.
- (7) Kivimäki, A.; Coreno, M.; Richter, R.; Alvarez Ruiz, J.; Melero García, E.; de Simone, M.; Feyer, V.; Vall-llosera, G.; Prince, K. C. Fluorescence Emission Following Core Excitations in the Water Molecule. *J. Phys. B: At., Mol. Opt. Phys.* **2006**, *39*, 1101–1112.
- (8) Melero García, E.; Kivimäki, A.; Pettersson, L. G. M.; Alvarez Ruiz, J.; Coreno, M.; de Simone, M.; Richter, R.; Prince, K. C. Fluorescence Emission of Excited Hydrogen Atoms after Core Excitation of Water Vapor. *Phys. Rev. Lett.* **2006**, *96*, No. 063003.
- (9) Carter, R. T.; Huber, J. R. Quantum Beat Spectroscopy in Chemistry. *Chem. Soc. Rev.* **2000**, *29*, 305–314.
- (10) Gallagher, T.F. Quantum-Beat, Level-Crossing, and Anticrossing Spectroscopy. In *Experimental Methods in the Physical Sciences* (Academic Press: New York, 1996), pp. 325–339, Vol 29B, Chap. 16.
- (11) Andrä, H. J. Stark-induced quantum beats in H LY_α emission. *Phys. Rev. A* **1970**, *2*, 2200–2207.
- (12) Leuchs, G.; Walther, H. Quantum Interference Effects in Field Ionization: Application to the Measurement of the Fine Structure Splitting of Highly Excited Na ^2D states. *Z. Phys. A* **1979**, *293*, 93–101.
- (13) Jeys, T. H.; Smith, K. A.; Dunning, F. B.; Stebbings, R. F. Investigation of Fine-Structure Quantum Beats in Sodium Rydberg Atoms by Field Ionization. *Phys. Rev. A* **1981**, *23*, 3065–3070.
- (14) Feynman, R.; Hollingsworth, J.; Vennettilli, M.; Budner, T.; Zmiewski, R.; Fahey, D. P.; Carroll, T. J.; Noel, M. W. Quantum Interference in the Field Ionization of Rydberg Atoms. *Phys. Rev. A* **2015**, *92*, No. 043412.

(15) Kivimäki, A.; Sankari, A.; Kettunen, J. A.; Stråhlman, C.; Álvarez Ruiz, J.; Richter, R. Field Ionization of High-Rydberg Fragments Produced after Inner-Shell Photoexcitation and Photoionization of the Methane Molecule. *J. Chem. Phys.* **2015**, *143*, 114305.

(16) Merkt, F.; Osterwalder, A.; Seiler, R.; Signorell, R.; Palm, H.; Schmutz, H.; Gunzinger, R. High Rydberg States of Argon: Stark Effect and Field-Ionization Properties. *J. Phys. B: At., Mol. Opt. Phys.* **1998**, *31*, 1705–1724.

(17) Kramida, A., Ralchenko, Yu., Reader, J., and NIST ASD Team (2019). *NIST Atomic Spectra Database* (ver. 5.7.1); National Institute of Standards and Technology, Gaithersburg, MD, 2020; <https://physics.nist.gov/asd> (accessed Oct 6, 2020).

(18) Prince, K. C.; Blyth, R. R.; Delaunay, R.; Zitnik, M.; Krempasky, J.; Slevak, J.; Camilloni, R.; Avaldi, L.; Coreno, M.; Stefani, G.; Furlani, C.; et al. The Gas-Phase Photoemission Beamline at Elettra. *J. Synchrotron Radiat.* **1998**, *5*, 565–568.

(19) Hikosaka, Y.; Lablanquie, P.; Shigemasa, E. Efficient Production of Metastable Fragments around the 1s Ionization Threshold in N₂. *J. Phys. B: At., Mol. Opt. Phys.* **2005**, *38*, 3597–3605.

(20) Armen, G. B. Spectator Excitation Accompanying Core Auger Decay in Atoms: a Hydrogenic Model. *J. Phys. B: At., Mol. Opt. Phys.* **1996**, *29*, 677–688.

(21) Kuchiev, M. U.; Sheinerman, S. A. Post-Collision Interaction in Atomic Processes. *Sov. Phys. Usp.* **1989**, *32*, 569–587.

(22) Hikosaka, Y.; Sawa, M.; Nakano, M.; Soejima, K.; Lablanquie, P.; Penent, F.; Ito, K. Electron Reemission Processes Following Photoelectron Recapture due to Post-Collision Interaction in inner-Shell Photoionization of Water Molecules. *J. Chem. Phys.* **2013**, *138*, 214308.

(23) Kivimäki, A.; Stråhlman, C.; Wasowicz, T. J.; Kettunen, J. A.; Richter, R. Yields and Time-of-Flight Spectra of Neutral High-Rydberg Fragments at the K Edges of the CO₂ Molecule. *J. Phys. Chem. A* **2016**, *120*, 4360–4367.

(24) Kivimäki, A.; Álvarez-Ruiz, J.; Sergio, R.; Richter, R. Production of Excited H atoms at the C 1s Edge of the Methane Molecule Studied by VUV-Photon-Photoion and Metastable-Fragment-Photoion Coincidence Experiments. *Phys. Rev. A* **2013**, *88*, No. 043412.

(25) Lejeune, A.; Chérigier-Kovacic, L.; Doveil, F. Lyman- α Radiation of a Metastable Hydrogen Beam to Measure Electric Fields. *Appl. Phys. Lett.* **2011**, *99*, 181502.

(26) Radchenko, V. I.; Ved'manov, G. D. Formation of Hydrogen Atoms in the 2s and 2p States by Neutralization of H⁻ Ions in Gases. *J. Exp. Theor. Phys.* **1995**, *80*, 670–679.

(27) Gemišić Adamov, M.; Steiger, A.; Grützmacher, K.; Seidel, J. Doppler-Free Stark Spectroscopy of the Second Excited Level of Atomic Hydrogen for Measurements of Electric Fields. *Phys. Rev. A* **2007**, *75*, No. 013409.

(28) Zimmerman, M. L.; Littman, M. G.; Kash, M. M.; Kleppner, D. Stark Structure of the Rydberg States of Alkali-Metal Atoms. *Phys. Rev. A* **1979**, *20*, 2251–2275.

(29) Gregoric, V. C.; Kang, X.; Liu, Z. C.; Rowley, Z. A.; Carroll, T. J.; Noel, M. W. Quantum Control via a Genetic Algorithm of the Field Ionization Pathway of a Rydberg Electron. *Phys. Rev. A* **2017**, *96*, No. 023403.

(30) Bailey, D. S.; Hiskes, J. R.; Riviere, A. C. Electric Field Ionization Probabilities for the Hydrogen Atom. *Nucl. Fusion* **1965**, *5*, 41–46.